A crystal optical study of phase transitions in $Sr_{1-x}Ba_xTiO_3$ single crystals

1996 J. Phys.: Condens. Matter 8 2377

(http://iopscience.iop.org/0953-8984/8/14/012)

J. Phys.: Condens. Matter **8** (1996) 2377–2388. Printed in the UK

A crystal optical study of phase transitions in $Sr_{1-x}Ba_xTiO_3$ single crystals

P A Markovin†, W Kleemann‡, R Lindner‡, V V Lemanov†,
O Yu Korshunov† and P P Syrnikov†

† A F Ioffe Physico-Technical Institute, Russian Academy of Sciences, St Petersburg 194021, Russia
‡ Angewandte Physik, Gerhard-Mercator-Universität Duisburg, D-47048 Duisburg, Germany

Received 30 November 1995

Abstract. The temperature variations of the refractive index and of the linear birefringence have been studied in flux-grown nominally pure $SrTiO_3$ and $Sr_{1-x}Ba_xTiO_3$ (SBT) single crystals ($x = 0.02$, 0.08 and 0.17) in the temperature range from 5 to 300 K. Polar domain structures were studied by polarizing microscopy. In SBT ($x = 0.17$) two phase transitions (PTs) at $T_{c1} = 91$ K (cubic, paraelectric-to-tetragonal, ferroelectric) and $T_{c2} = 76$ K (to orthorhombic or rhombohedral) were detected. SBT ($x = 0.08$) undergoes a PT at $T_c = 50$ K (cubic, paraelectric-to-orthorhombic or rhombohedral, ferroelectric). In the low-x limit ($x = 0.02$) the cubic-to-tetragonal PT of pure $SrTiO_3$ was observed at $T_0 = 70$ K. Below $T_c = 28$ K a polar state with C_{2v} symmetry and weak anisotropy was observed. Contributions of the spontaneous electro-optic effect to the temperature variation of the refractive index in SBT ($x = 0.08$ and 0.17) allow us to estimate the spontaneous polarization and its temperature variation.

1. Introduction

The perovskite-type incipient ferroelectric or quantum paraelectric strontium titanate ($SrTiO_3$, henceforth denoted as STO) is very sensitive to doping with impurities because of its highly polarizable lattice [1]. Substituting for Sr^{2+} ions with small amounts of Ca^{2+} or Ba^{2+} leads to ferroelectric phase transitions (PTs) at low temperatures, T [2–6]. Unlike the $Sr_{1-x}Ca_xTiO_3$ system (SCT for short) [2], solid solutions $Sr_{1-x}Ba_xTiO_3$ (SBT for short) with $x > 0.2$ [6] undergo a sequence of PTs upon cooling similar to that observed in nominally pure $BaTiO_3$ [7, 8], namely: paraelectric, cubic (O_h)-to-ferroelectric, tetragonal (C_{4v})-to-orthorhombic (C_{2v})-to-rhombohedral (C_{3v}). Despite the rather long history of investigations on SBT most experimental research was done on samples with high concentration of Ba^{2+} ($x > 0.5$) and mainly on ceramics. There are only a few studies concerned with low-T properties of SBT in the low-x limit ($x \leqslant 0.016$) [3–6]. In particular, detailed investigations of the PTs for $x < 0.2$ are lacking. Recently [7] we have been able to show that this range of x displays, in fact, quite interesting novel features. Evidence was found that SBT undergoes a low-T transformation from ferroelectric to glassy behaviour similar to that known of for SCT and for the related impurity systems $KTaO_3$:Li and $KTaO_3$:Nb [8]. Up to now, at which value of x the crossover takes place from $BaTiO_3$-type (with three ferroelectric phases) into STO-type (with only one polar low-T phase) behaviour has been unknown.

In order to clarify the phase transformations in SBT for relatively small concentrations of Ba^{2+} we have investigated the temperature variation of the refractive index (RI) and

0953-8984/96/142377+12$19.50

the temperature and electrical field dependences of the linear birefringence (LB) in SBT single crystals with $x = 0$, 0.02, 0.08 and 0.17. Additionally, measurements of the transmitted light intensity were made. A preliminary study of domain structures at the points of transformations was carried out simultaneously with the refractometric measurements. They allow us to obtain the temperatures of the ferroelectric PTs, to evaluate the value of spontaneous polarization in the samples under study and to conclude that the permittivity of SBT with $x = 0.02$ has a fairly low anisotropy, unlike that of SCT.

2. Experimental procedure

Single crystals of the solid solutions $SrTiO_3$–$BaTiO_3$ were grown by the flux method. The concentrations of Ba^{2+} were determined by x-ray lattice constant measurements using Vegard's law. Comparison with the dielectric response of ceramics with well known compositions [6] showed good agreement for $x = 0.02$ and slight deviations for $x = 0.08$ and 0.17, where the ceramics indicate $x = 0.065$ and 0.135, respectively.

Nominally pure STO and SBT ($x = 0.02$) samples with edges a, b and c along the cubic directions $[110]_c$, $[1\bar{1}0]_c$ and $[001]_c$ and c/a and $c/b \approx 2$–3, were polished to optical quality. These directions refer to the tetragonal axes a, b and c, respectively, below the temperature of the antiferrodistortive (O_h–D_{4h}) PT, $T_0 = 105$ K, for STO. Since it has been shown [4] that SBT with low x undergoes a structural cubic-to-tetragonal PT similar to that in STO, the above orientation and size guaranteed that the samples formed a structural single domain [9]. The SBT samples with $x = 0.08$ and 0.17 were cut along the cubic $\langle 100\rangle$ directions. Refractometric measurements of SBT ($x = 0.02$) were also made for samples with $\{100\}$ faces. All of the SBT samples revealed internal stress, which was clearly seen at room temperature under a polarizing microscope.

The temperature dependences of the RIs were measured at the wavelength 632.8 nm of a He–Ne laser in the temperature range from 20 to 300 K using a homodyne-type interferometer [10]. The sensitivity of this technique is $\delta n \approx 10^{-6}$ at an absolute accuracy of about 10^{-5}. The advantages of the method are its very low variation of sensitivity with respect to changes of the light intensity transmitted by the sample, as well as low sensitivity to the influence of the depolarization of light passed through the sample. The technique allows us to measure variations of the optical phase difference or the specific optical retardation $\delta\psi(T)$, which is related to the variation of the RI, $\delta n(T)$, and to the linear sample dilation, $\delta L(T)/L$, along the propagation direction:

$$\delta\psi(T) = \delta n(T) + (n+1)\,\delta L(T)/L. \tag{1}$$

Lacking data on the temperature dependence of the lattice parameters of SBT, we did not attempt to separate dilation from refractive effects in our phase-shift measurements. Additionally the transmitted light intensity I_{tr} through the SBT samples placed between crossed polarizers was measured at the He–Ne laser wavelength.

The LB was measured on selected areas with size 80 × 80 μm. In SBT ($x = 0.02$) light was propagated along the b-axis in order to measure the principal LB, Δn_{ac}. For SBT ($x = 0.08$) the polarizers were parallel either to $[110]_c$ or to $[100]_c$, and for SBT ($x = 0.17$) they were parallel to $[110]_c$. Temperatures between 5 and 300 K were achieved using a He evaporation cryostat allowing temperature control to within $\delta T \approx \pm 0.05$ K. An electric bias field up to 250 kV m^{-1} was applied in the LB measurements using silver paste electrodes. Simultaneously with the investigation of the LB the appearance and transformation of domain structure in the SBT samples were checked using a polarizing microscope.

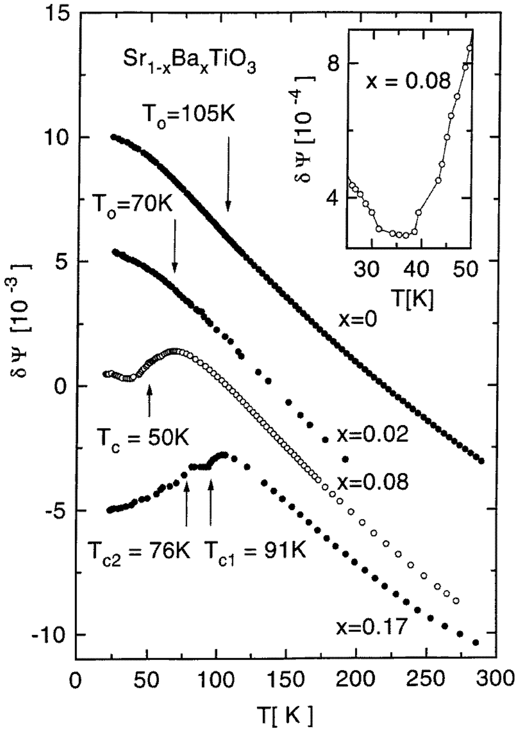

Figure 1. Optical retardation curves, $\delta\psi$ versus T, arbitrarily shifted against one another, for nominally pure $SrTiO_3$ and for $Sr_{1-x}Ba_xTiO_3$ ($x = 0.02$, 0.08, 0.17). Inset: details of $\delta\psi$ versus T for SBT ($x = 0.08$). Transition temperatures are indicated by arrows.

3. Experimental results and discussion

3.1. SBT ($x = 0.08$ and 0.17)

In figure 1 the T-dependences of the optical retardation $\delta\psi(T)$ in SBT are shown. For STO we present only $\delta\psi(T)$, because of the small difference between $\delta\psi_c(T)$ and $\delta\psi_a(T)$ in nominally pure strontium titanate. A minute change of slope of $\delta\psi(T)$ for STO at $T_0 = 105$ K, similar to what was observed previously [11], indicates the structural PT into the low-T tetragonal phase.

The decrease of $\delta\psi(T)$ for SBT ($x = 0.08$ and 0.17) at low temperatures in comparison with the monotonic behaviour found in STO is attributable to the contribution of spontaneous polarization via the electro-optical effect. In SBT ($x = 0.08$) a bending point referring to a maximum of $\mathrm{d}\,\delta\psi(T)/\mathrm{d}T$ is found at $T_c \approx 50$ K. Below 50 K we observe the appearance of a domain structure with domain walls along $\langle 100\rangle_c$ directions and size $\leqslant 50$ μm. The direction of the domain walls does not change with decreasing temperature, but in the range from 30 to 50 K domain wall motion is microscopically observed during cooling and heating procedures.

In SBT ($x = 0.17$) there are two kink-like anomalies indicated at $T_{c1} \approx 91$ K and $T_{c2} \approx 76$ K. Preliminary measurements of the temperature dependence of the dielectric permittivity show a peak at T_{c1} and a step-like anomaly near to T_{c2}. Pronounced anomalies at T_{c1} and T_{c2} are also present in the temperature dependence of the LB (figure 2, curve 3). Similarly to in SBT ($x = 0.08$), domains with walls along $\langle 110\rangle_c$ directions and with size $\leqslant 50$ μm appear below T_{c1}. Below T_{c2} a change of the domain pattern is observed with new directions of the domain walls along the $[100]_c$ axes. They become particularly clear-cut on cooling under a moderate electric field, $E \approx 50$ kV m^{-1}, parallel to $[100]_c$,

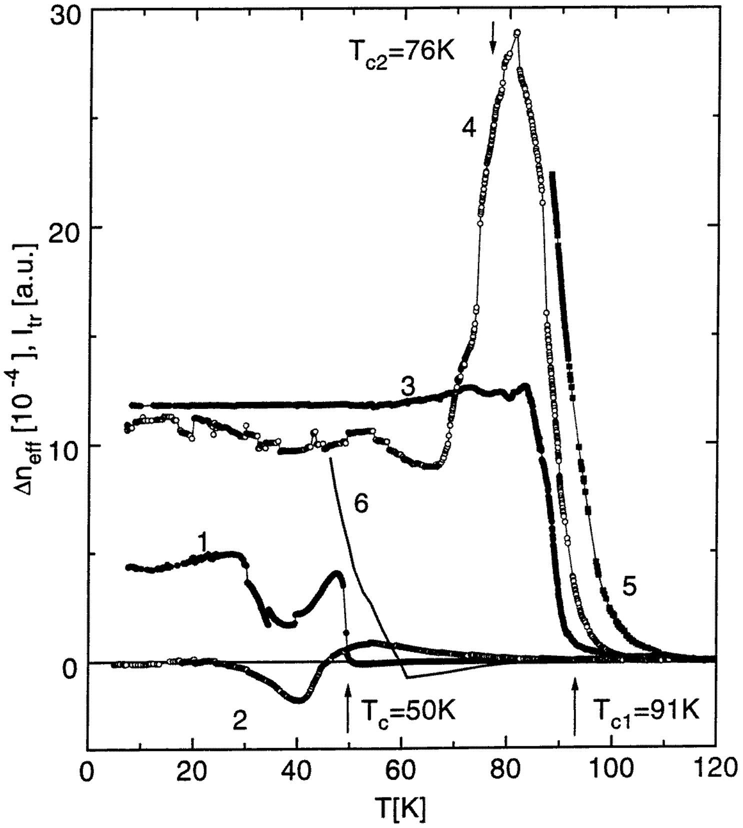

Figure 2. Temperature dependences of the effective values of the LB measured at zero external field for SBT ($x = 0.08$) with polarizers parallel to $[100]_c$ (curve 1) and $[110]_c$ (curve 2), respectively, and for SBT ($x = 0.17$) with polarizers parallel to $[110]_c$ (curve 3), upon zero-field heating after field cooling (curve 4) and upon field cooling with $E_{ext} = 129$ kV m^{-1} (curve 5). Curve 6 shows the light intensity transmitted by SBT ($x = 0.08$) placed between crossed polarizers. Transition temperatures are indicated by arrows.

and are preserved down to lowest temperatures. The transformation of the domain structure observed under a polarizing microscope is confirmed by imaging diffraction patterns of laser light due to irregular domain wall gratings.

According to our observations the SBT system very probably reveals domain formation processes similar to those observed in nominally pure $BaTiO_3$. For the tetragonal phase of $BaTiO_3$ in a (001) plate, a 90° domain structure with walls along the $[110]_c$ direction is very typical [12–16]. Even if *ac*-domain walls, i.e. walls parallel to [100] directions, are observed, in addition walls parallel to [110] directions are also present. This corroborates our assumption that SBT ($x = 0.17$) undergoes a ferroelectric PT into a tetragonal C_{4v} phase at $T_{c1} = 91$ K.

Experimental data on domain structures in the orthorhombic and rhombohedral phases of $BaTiO_3$ are very poor [12, 13, 16]. In the orthorhombic phase of a (100) plate, 90° domains with walls along the $\langle 101\rangle_c$ directions and 60° domains with walls along the $[100]_c$ and $[110]_c$ directions within the (100) plane are observed. In the rhombohedral phase domains with walls along the $[100]_c$ direction are known. Taking into account that domain walls along the $[100]_c$ direction are observed in SBT ($x = 0.08$) below $T_c = 50$ K and in SBT ($x = 0.17$) below $T_{c2} = 76$ K, we are inclined to assume orthorhombic or rhombohedral phases in both types of sample below these temperatures.

Thus all of the optical measurements for SBT ($x = 0.08$ and 0.17) below T_c and T_{c1}, respectively, were performed on ferroelectric polydomain samples. Quite frequently erratic jumps of the LB signal are encountered. They are due to irregular domain wall motion (see above). LB measurements, hence, do not reflect directly the difference between principal values of refractive indices. They are thus less promising for quantitative analysis. Nevertheless, the appearance of particularly large changes, $\delta\,\Delta n$, of the LB signal (figure 2, curve 1 at ≈50 K and curve 3 at ≈91 K) strongly hints at the occurrence of PTs from cubic to low-T ferroelectric phases at these temperatures. The effective value of the LB in SBT ($x = 0.17$), measured with polarizers parallel to $[110]_c$, does not change significantly during various temperature cycles through T_{c1} at zero external field (figure 2, curve 3). Obviously, by virtue of some quenched stress distribution the domain pattern is reproduced upon cycling through the PT, thus leaving the LB signal invariant. After cooling the sample in an electric field applied along the $[100]_c$ direction and making measurements on it subsequently upon zero-field heating, the LB is found to have increased by more than a factor of two in the temperature range just below $T_{c1} = 91$ K (figure 2, curve 4). Obviously the direction of the external field is parallel to the easy direction of the spontaneous polarization in the proposed C_{4v} phase. Cooling in an electric field (figure 2, curve 5) yields a similar effect, but the onset of ferroelectricity appears at higher temperature, as expected. Measurements of the LB below $T = 88$ K in an electrical field are not shown because of their noise due to unreproducible domain motion.

For SBT ($x = 0.08$) the temperature dependence of the LB complies well with orthorhombic or rhombohedral symmetry below $T_c = 50$ K, where the direction of polarization lies along $[110]_c$ or $[111]_c$ as deduced from our domain structure analysis. As revealed by measurements with polarizers parallel to $[100]_c$ the LB peak starts to grow below T_c (figure 2, curve 1). On the other hand, Δn_{eff}, measured with polarizers parallel to $[110]_c$, nearly vanishes in the vicinity of T_c (figure 2, curve 2).

An additional anomaly of the LB appears for SBT ($x = 0.08$) near $T = 40$ K. Whereas in $[110]_c$ geometry Δn_{eff} increases, it decreases in $[100]_c$ geometry. This is consistent with an anomaly of the temperature dependence of the average RI (figure 1, inset). At approximately the same temperature a small step-like anomaly is observed in the temperature dependence of the dielectric permittivity of SBT ceramics ($x = 0.06$ and 0.09), which is associated with another ferroelectric PT near 40 K [17]. We do not observe any changes of the domain wall directions around 40 K, but intense domain motion in the region from 30 to 50 K is clearly seen upon both cooling and heating. In contrast with the readily reproducible increase of Δn_{eff} in $[100]_c$ geometry below T_c, the size and the temperature position of the LB anomaly near 40 K are less reproducible. Nevertheless, we cannot exclude the possibility of the presence of a PT from orthorhombic to rhombohedral symmetry, assuming similar domain patterns of both phases to appear in the $(100)_c$ plane. On the other hand, some interaction of true ferroelectric domains with quantum paraelectric state clusters cannot be excluded. The latter are believed to appear near this temperature in nominally pure STO [18]. Hence, domain wall motion coupled with anomalies of optical and dielectric properties might be involved.

In this last case we conjecture that only one ferroelectric PT is present in SBT ($x = 0.08$) (cubic to orthorhombic or rhombohedral), but at least two ferroelectric phases (tetragonal and orthorhombic or rhombohedral) are detected in SBT ($x = 0.17$). As shown previously [6], a sequence of three ferroelectric PTs (cubic–tetragonal–orthorhombic–rhombohedral) is found for SBT with $x > 0.2$. It is, hence, reasonable to assume the presence of multicritical points, where the above sequence coalesces first into two PTs ($0.17 < x < 0.20$) and finally into one PT ($0.08 < x < 0.17$). The situation thus resembles that observed for $KTa_{1-x}Nb_xO_3$, where the three-transition sequence collapses into a single transition for $0.02 < x < 0.03$ [19]. If this situation is applicable to SBT, too, another PT remains to be discovered for SBT ($x = 0.17$), very probably at temperatures slightly below $T_{c2} = 76$ K. Owing to blurring by multidomains, the situation cannot be clarified on the basis of our present LB data.

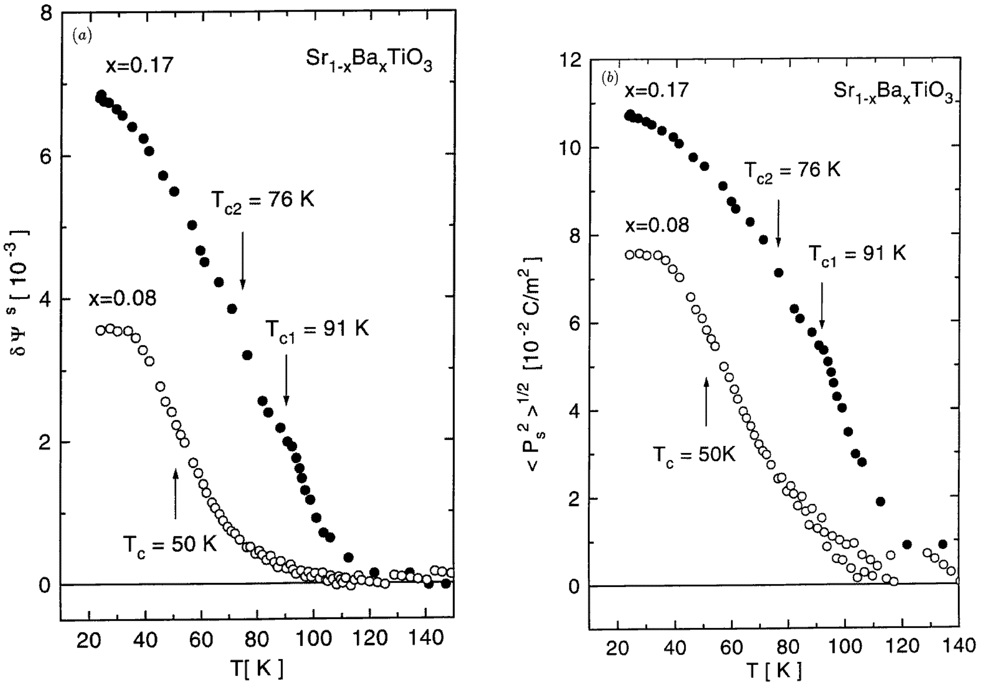

(*a*) (*b*)

Figure 3. Spontaneous contributions to the optical retardation (*a*) leading to autocorrelation functions of the polarization (*b*) in SBT ($x = 0.08$ and 0.017) as functions of the temperature. Transition temperatures are indicated by arrows.

In order to evaluate the ferroelectric contributions to the variations of the optical retardation of SBT in figure 1 it is necessary to find a reliable approximation for the non-ferroelectric (regular) behaviour of the refraction. As is well known this varies due to thermo-optical and photoelastic mechanisms [10] as was confirmed, e.g., for pure STO [11, 20]. As is seen in figure 1 the temperature dependence of $\delta\psi(T)$ for nominally pure STO is very similar to that for the paraelectric phase SBT samples well above T_c. This suggests the use of STO as a reference material for evaluating the regular behaviour of the temperature variation of $\delta\psi(T)$ for SBT. We thus obtain the ferroelectric contribution to the optical retardation, $\delta\psi^s(T)$, for SBT as the difference between $\delta\psi(T)$ for STO samples and that for SBT samples as shown in figure 3(*a*).

Before we discuss the ferroelectric contribution to the optical retardation of SBT it is necessary to note that the change of $\delta\psi(T)$ depends on the changes of both the RI and the dilation; see equation (1). Thus when using the expression 'refraction of light' we include both contributions in $\delta\psi(T)$. Since for pure $SrTiO_3$ the relative change of the RI with temperature $\delta n(T)$ is equal to $\delta\psi(T)$ within an error of about 20% [11], one may assume $\delta\psi^s \approx \delta n^s$ also for SBT.

Table 1. Effective electro-optical coupling coefficients describing coupling between the principal refractive indices n_i and the autocorrelation function $\langle P_s^2\rangle$ according to equation (2) and [21] for various phases of $Sr_{1-x}Ca_xTiO_3$, $x \ll 1$.

	Electro-optical coupling coefficients A_{i3} (m^4 C^{-2})		
Principal refractive index	Tetragonal	Orthorhombic	Rhombohedral
n_3	−1.02	−0.92	−0.89
n_2	−0.27	−0.31	−0.34
n_1	−0.27	−0.27	−0.34

The ferroelectric contribution $\delta\psi^s \approx \delta n^s$ to the principal values of the refractive indices n_i arises from the autocorrelation function of the polarization $\left\langle P_s^2\right\rangle$ [21, 22]:

$$\delta\psi_1^s \approx \delta n_1^s = -(n_i^3/2)g_{i3}^*\left\langle P_s^2\right\rangle = A_{i3}\left\langle P_s^2\right\rangle \tag{2}$$

where g_{i3}^* are second-order polarization optical coefficients and $\left\langle P_s^2\right\rangle$ is assumed to refer to the spontaneous polarization, P_s, lying along the axis indexed as 3. The electro-optic coefficients in the ferroelectric phases, g_{i3}^*, are related to the coefficients g_{ij} in the paraelectric centrosymmetric phase according to a relationship derived in [21]. Assuming that introduction of small numbers of Ba^{2+} ions does not significantly change g_{ij} for nominally pure STO, we have calculated the coefficients A_{i3} in equation (2) for the tetragonal, orthorhombic and rhombohedral ferroelectric phases in SBT using $n_1 \approx n_0 \approx 2.38$, $g_{11} \approx 0.15$ m^4 C^{-2}, $g_{12} \approx 0.04$ m^4 C^{-2} and $g_{44} = 0.08$ m^4 C^{-2} for STO [23]. All coefficients are assumed to be temperature independent [24]. The results are shown in table 1.

Since we measured the optical retardation for polydomain samples in ferroelectric phases, the optical retardations $\delta\psi(T)$ at low temperatures and, hence, the ferroelectric contributions $\delta\psi^s \approx \delta n^s$ (figure 3(*a*)) contain values averaged over the contributions of all domains along the direction of the light beam propagation. It seems, hence, justified within the optical indicatrix perturbation approach to evaluate the data of figure 3(*a*) by using averaged coupling coefficients, which we approximate by $A_{av} = -0.6$ m^4 C^{-2} in the orthorhombic and rhombohedral ferroelectric phases. The spontaneous polarizations in SBT ($x = 0.08$ and 0.17) thus obtained from equation (2) using $\delta\psi_{av}^s$ from figure 3(*a*) are shown in figure 3(*b*). We find $P_s \approx 7 \times 10^{-2}$ C m^{-2} and 11×10^{-2} C m^{-2} for SBT ($x = 0.8$ and 0.17, respectively), in reasonable agreement with $P_s \approx 25 \times 10^{-2}$ C m^{-2} for pure $BaTiO_3$ considering that T_c decreases in SBT with decreasing Ba^{2+} concentration [6].

It is seen from figures 3(*a*) and 3(*b*) that ferroelectric precursor contributions to the RI of SBT ($x = 0.08$ and 0.17) appear at temperatures 50–60 K above T_c. Because of the isotropic character of the precursor contribution in the cubic phase it is clearly seen in $\delta\psi^s$ versus T (figure 3(*a*)). The LB (figure 2) reflects the anisotropy of the precursor polarization only by virtue of coupling to internal stress fields [25]. Precursor processes were also observed in the temperature dependence of the light intensity I_{tr} transmitted through SBT samples placed between crossed polarizers. I_{tr} is a measure of the depolarization of light. For SBT ($x = 0.08$) a drastic increase of I_{tr} is observed at $T \approx 60$ K (figure 2, curve 6) for incident light with $[110]_c$ polarization. This might be connected with the growth of polarization clusters comparable with the wavelength of light and coupling to internal stress. In agreement with this assumption the precursor LB in $[110]_c$ geometry also achieves relatively high values around 60 K (figure 2, curve 2). Near to $T_c = 50$ K only a change of slope is observed for $I_{tr}(T)$. For SBT ($x = 0.17$) I_{tr} starts to increase at T_{c1}.

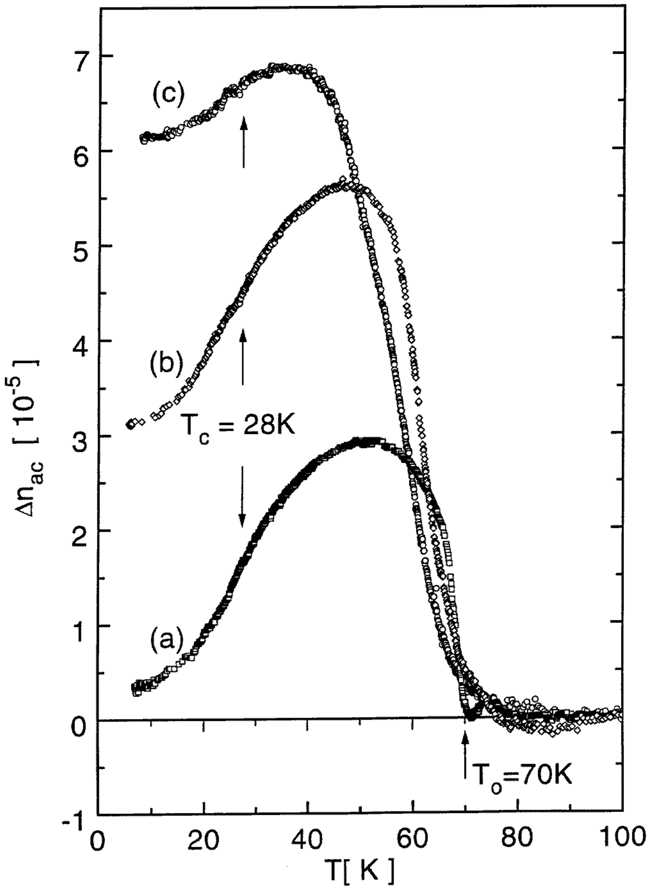

Figure 4. Temperature dependences of Δn_{ac} for SBT ($x = 0.02$) measured on different sample areas. Transition temperatures are indicated by arrows.

3.2. SBT ($x = 0.02$)

A change of slope of $\delta\psi(T)$ for SBT ($x = 0.02$) at $T_0 = 70$ K (figure 1) indicates the structural PT to the low-T tetragonal phase, similar to that in STO, at $T_0 = 105$ K. The transition temperature agrees with a linear extrapolation of its dependence on the Ba^{2+} concentration deduced from elastic compliance measurements for SBT ($x \leqslant 0.014$) [4]. More clearly T_0 is indicated by the LB measurements shown in figure 4, where Δn_{ac} abruptly sets in just below T_0. In contrast with the case for SBT ($x = 0.08$ and 0.17) no structural domains were observed under the polarizing microscope for $T < T_0$. Nevertheless, the observed dependence of Δn_{ac} on the sample position clearly seems to indicate multidomain effects. When comparing our LB data with those obtained by Bednorz on a carefully prepared single-domain sample of SBT ($x = 0.016$) with $T_0 = 75$ K and $\Delta n_{ac}(40\text{ K}) \approx 1.1 \times 10^{-4}$ [5], we conjecture that curve (c) with $\Delta n_{ac}(40\text{ K}) \approx 0.7 \times 10^{-4}$ comes closest to a crystallographic single domain.

At temperatures $T_1 < T_0$, the principal LB, $|\Delta n_{ac}|$, decreases smoothly and bends into a horizontal low-T tail after passing a point of inflexion at $T_c \approx 28$ K (figure 4). This effect is most pronounced in curve (a), where $T_1 \approx 65$ K. Weaker anomalies are found in curves (b) and (c), where $T_1 \approx 45$ and 40 K, respectively. These anomalies are very probably related to a low-T polar phase similar to that observed for SCT [2, 26]. Contrastingly with the case for SCT, however, in our measurements the polar anomaly is different in sign compared with the structural one, which is due to the tetragonal elongation along the c-axis in both SCT and SBT. On the other hand, Bednorz's sample of SBT ($x = 0.016$) [5] shows a large positive polar anomaly, growing up to $\delta\,\Delta n_{ac} \approx 1.3 \times 10^{-3}$ from 30 to 5 K and, hence, resembling that for SCT [26] to a large extent. We argue that the different behaviours of the samples are due to the different orientations of the polarization within the more or less perfect tetragonal single domains. Whereas a positive sign of $\delta\,\Delta n_{ac}$ indicates that the polarization lies in plane, $\boldsymbol{P} \parallel [110]_c$, $\delta\,\Delta n_{ac} < 0$ very probably signifies perpendicular orientation, $\boldsymbol{P} \parallel [1\bar{1}0]_c$. Presumably internal stress lies at the origin of the different orientations. The SBT ($x = 0.016$) sample [5] was carefully annealed at 1800 °C prior to lapping, which merely induces perpendicular compressive stress and orientates $\boldsymbol{P}$ parallel to the plane, $P_s = \langle P_a \rangle$. On the other hand, our sample was heavily stressed along arbitrary directions due to the growth process. In-plane tensile components then cause reorientation of $\boldsymbol{P}$ perpendicular to the plane, $P_s = \langle P_b \rangle$ [5].

This situation can be taken into account via a simple indicatrix calculation [27]. We start from the cubic phase, introduce the strains e_3 and e_1 due to the structural instability at T_0 and the polarization correlation functions $\langle P_i P_j \rangle$, $i, j = x, y$ and z. Bearing in mind the rotation of the crystal axes when changing from cubic to low-T symmetry (tetragonal and orthorhombic, respectively), we expect spontaneous components $\langle P_x \rangle = \pm \langle P_y \rangle = \pm P_s/2$ for $\boldsymbol{a}$- and $\boldsymbol{b}$-domains, respectively. Furthermore we have $\langle P_x P_y \rangle = \pm P_s^2/2$ and $\langle P_x^2 \rangle = \langle P_y^2 \rangle \neq \langle P_z^2 \rangle$. The volume fractions referring to $\boldsymbol{a}$- and $\boldsymbol{b}$-orientated polarization are taken into account via the adjustable parameters $1 - \alpha$ and α, respectively. Straightforward calculation yields the $[110]_c$-plane LB:

$$\begin{aligned}\Delta n_{ac} &= n_c - n_a = \delta_{\text{struct}}\,\Delta n_{ac} + \delta_{\text{pol}}\,\Delta n_{ac} \\ &= (n_0^3/2)\left[(p_{11} - p_{12})(e_1 - e_3) + (g_{11} - g_{12})\left(\langle P_x^2 \rangle - \langle P_z^2 \rangle\right) + (\tfrac{1}{2} - \alpha) g_{44} P_s^2\right].\end{aligned} \tag{3}$$

Since $e_3 > e_1$ and $p_{11} < p_{12}$, the strain-induced LB, $\delta_{\text{struct}}\,\Delta n_{ac}$, is positive, whereas the polarization-induced LB, $\delta_{\text{pol}}\,\Delta n_{ac}$, may change sign depending on the value of α. The case where $\alpha = 0$ yields $\delta_{\text{pol}}\,\Delta n_{ac} > 0$ as always observed for SCT [5, 25] and for virtually stress-free SBT, where $\Delta n_{ac} \approx 1.37 \times 10^{-3}$ [5]. On the other hand, $\alpha = 1$ yields $\delta_{\text{pol}}\,\Delta n_{ac} < 0$ resulting in $\Delta n_{ac} \approx 6 \times 10^{-5}$ as observed in the extreme case of figure 4, curve (c). From these limiting values we easily calculate $P_s = 4.9 \times 10^{-2}$ C m^{-2} and $\langle P_z^2 \rangle^{1/2} \approx 2.1 \times 10^{-2}$ C m^{-2} by adding and subtracting equation (3) with $\alpha = 0$ and 1, respectively, using the low-T approximation $\langle P_x^2 \rangle = P_s^2/2$, and inserting the extrapolated value $\delta_{\text{struct}}\,\Delta n_{ac}(T \to 0) \approx 1.25 \times 10^{-4}$. It is noticed that the spontaneous polarization is somewhat larger than that obtained for SCT ($x = 0.011$), $P_s \approx 2.9 \times 10^{-2}$ C m^{-2} [26].

The large negative LB anomaly occurring in samples with perpendicular polarization clearly hints at important $\boldsymbol{z}$-directed polarization fluctuations $\langle P_z^2 \rangle$. These are usually neglected in SCT [26] because of its low ε_c-value [2]. In SBT, however, the anisotropy of the permittivity is much smaller, $\varepsilon_c \approx \varepsilon_a$ [4]. This is certainly connected with the large size

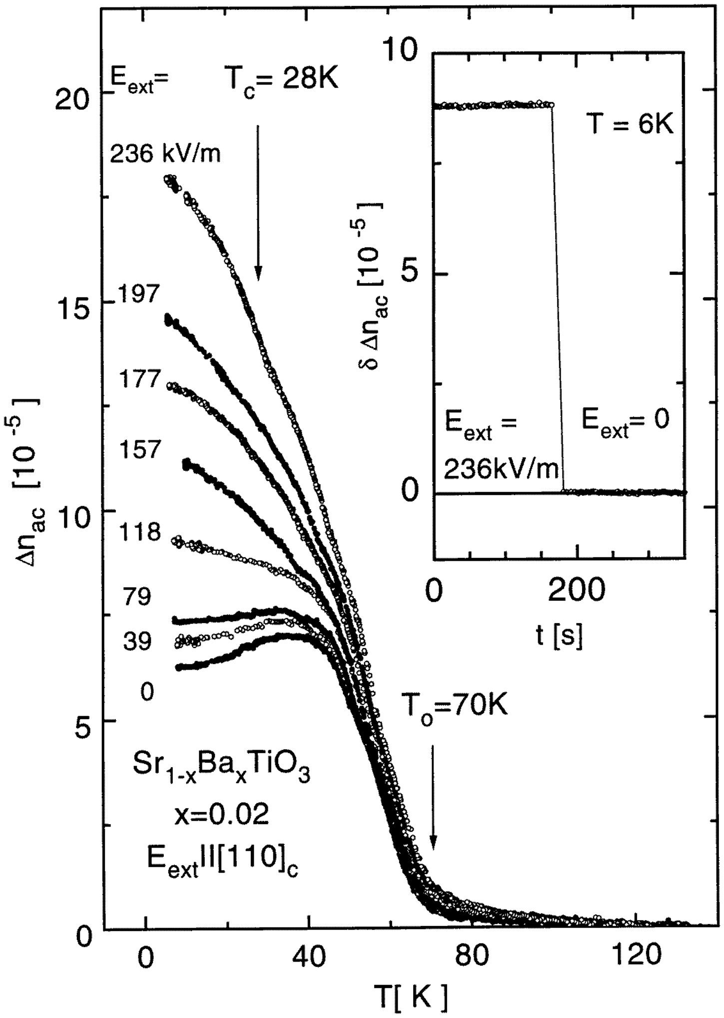

Figure 5. Temperature dependences of the principal birefringence Δn_{ac} of SBT ($x = 0.02$) under an external electric field applied along the $[110]_c$ direction. Inset: the time dependence of the electric-field-induced contribution to Δn_{ac} at $T = 6$ K after field cooling with $E = 236$ kV m^{-1} switched off at $t = 164$ s.

of the Ba^{2+} ion, which does not necessarily occupy a well defined off-centre position in the xy-plane, as Ca^{2+} does in SCT. Presumably it has a tendency to displace along $\boldsymbol{z}$ similarly to in the tetragonal phase of BaTiO$_3$. This view is corroborated by our measurements of the LB induced by an electrical field along $[110]_c$ (figures 5 and 6, curve 1) and along $[001]_c$ (figure 6, curve 2), respectively. Quadratic dependences $\delta\ \Delta n_{ac} \propto E^2$ are observed (solid lines), which indicate that the field effect can be treated in the paraelectric approximation when calculating $\delta_{\mathrm{pol}}\ \Delta n_{ac}$ from equation (3) with $P_j = \langle P_j \rangle + \varepsilon_0 \varepsilon_j E_j$, $j = \boldsymbol{c}$ or $\boldsymbol{a}$:

$$(\delta_{\mathrm{pol}}\ \Delta n_{ac})_{\boldsymbol{E}\|a} \approx (n_0^3/4)(g_{11} - g_{12} + g_{44})(\varepsilon_0 \varepsilon_a E_a)^2 \qquad (4a)$$

$$(\delta_{\mathrm{pol}}\ \Delta n_{ac})_{\boldsymbol{E}\|c} \approx -(n_0^3/2)(g_{11} - g_{12})(\varepsilon_0 \varepsilon_c E_c)^2. \qquad (4b)$$

Here we assume that the terms linear and quadratic in both $\langle P_a \rangle$ and $\langle P_c \rangle$ may be neglected,

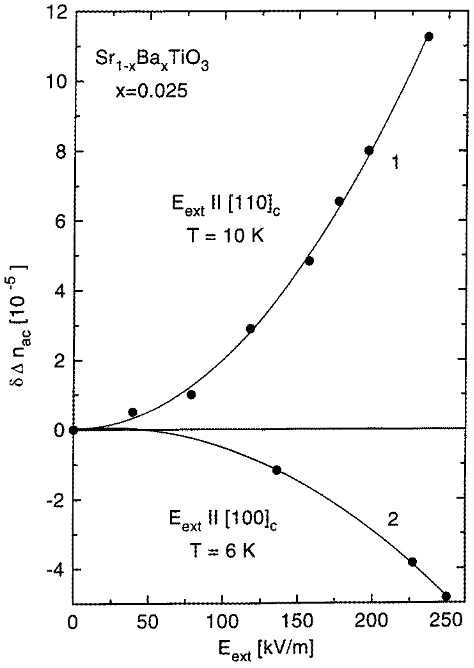

Figure 6. Electric-field-induced contributions to Δn_{ac} of SBT ($x = 0.02$) with $\boldsymbol{E}_{ext} \parallel [110]_c$ at $T = 10$ K (curve 1) and with $\boldsymbol{E}_{ext} \parallel [001]_c$ at $T = 6$ K (curve 2). Solid circles: experimental data points; lines: best-fitted E^2 curves.

since only $\langle P_b \rangle$ is non-vanishing (figure 5), before taking the data shown in figure 6. On this basis we calculate the values $\varepsilon_a = 6.3 \times 10^3$ and $\varepsilon_c = 5.1 \times 10^3$, which are of the same order of magnitude as reported for low T for SBT ($x = 0.014$): $\varepsilon_a \approx 1.8 \times 10^4$ and $\varepsilon_c \approx 1.4 \times 10^4$ [4]. It would be very interesting to study more precisely both the permittivity components and the LB for perfect single-domain samples.

The nature of the ferroelectric phase for $T < T_c \approx 28$ K is as yet unclear. Relatively sharp peaks of the dielectric permittivity [4, 5] indicate a ferroelectric PT. Similarly to the case of SCT, one might expect a disordered nanodomain state owing to the interaction with quenched random fields [2, 19, 26]. In contrast to the case of SCT, however, owing to the weak anisotropy of its permittivity SBT is a candidate for a Heisenberg rather than for an XY-model system [2]. Clearly, more careful experiments on better defined samples including measurements of low-frequency permittivity and second-harmonic generation are required for a better understanding of the SBT system in the low-x limit.

4. Conclusion

Various optical methods used in present study have shown that SBT with a Ba^{2+} content of $x = 0.17$ undergoes at least two ferroelectric PTs at $T_{c1} = 91$ K from a paraelectric, cubic to a ferroelectric, tetragonal phase and, at $T_{c2} = 76$ K, to an orthorhombic (or rhombohedral) phase. For SBT ($x = 0.08$) a ferroelectric PT at $T_c = 50$ K to an orthorhombic (or rhombohedral) phase is detected. A spontaneous ferroelectric contribution to the refraction of light is observed for SBT ($x = 0.08$ and 0.17). This allows us to estimate the value of the spontaneous polarization.

Analysis of the temperature and the electrical field dependences of the LB in SBT ($x = 0.02$) reveals that the spontaneous polarization lies in the plane perpendicular to the tetragonal c-axis, but appreciable polarizability is also found along the $\boldsymbol{c}$-direction. Future research needs to show whether or not the ferroelectric state is disordered on a nanoscale due to the influence of intrinsic random fields as in the case of SCT.

Acknowledgments

Thanks are due to U Bianchi for valuable discussions and technical help. This research was supported by NATO through Collaborative Research Grant No 930486.HTECH, the International Science Foundation and the Deutsche Forschungsgemeinschaft.

References

[1] Müller K A and Burkard H 1979 *Phys. Rev.* B **19** 3593
[2] Bednorz J G and Müller K A 1984 *Phys. Rev. Lett.* **52** 2289
[3] Hegenbarth E 1965 *Phys. Status Solidi* **9** 191
[4] Miura S, Marutake M, Unoki H, Uwe H and Sakudo T 1975 *J. Phys. Soc. Japan.* **38** 1056
[5] Bednorz J G 1982 *PhD Thesis* Swiss Federal Institute of Technology, Zürich
[6] Lemanov V V, Smirnova E P and Tarakanov E A 1995 *Fiz. Tverd. Tela* **37** 2476
[7] Markovin P A, Lemanov V V, Korshunov O Yu, Syrnikov P P, Bianchi U, Lindner R and Kleemann W 1996 *Ferroelectrics* at press
[8] Vugmeister B E and Glinchuk M D 1990 *Rev. Mod. Phys.* **62** 993
[9] Müller K A, Berlinger W, Capizzi M and Gränicher H 1970 *Solid State Commun.* **8** 549
[10] Markovin P A and Pisarev R V 1979 *Sov. Phys.–JETP* **50** 1190
[11] Kleemann W and Schäfer F J 1985 *Japan. J. Appl. Phys. Suppl.* 2 **24** 260
[12] Jona F and Shirane G 1972 *Ferroelectric Crystals* (New York: Pergamon) p 153
[13] Smolensky G A, Bokov V A, Isupov V A, Krainik N N, Pasynkov P E, Sokolov A I and Yushin N K 1985 *Physics of Ferroelectric Phenomena* (Leningrad: Nauka) pp 16, 195, 291 (in Russian)
[14] Merz W J 1954 *Phys. Rev.* **95** 690
[15] Park B M and Chung S J 1994 *Ferroelectrics* **157** 27
[16] Forsbergh P W 1949 *Phys. Rev.* **76** 1187
[17] Roth P, Hegenbarth E, Müller M and Escher U 1987 *Ferroelectrics* **74** 331
[18] Müller K A, Berlinger W and Tosatti E 1991 *Z. Phys.* B **84** 277
[19] Kleemann W 1993 *Int. J. Mod. Phys.* B **7** 2469
[20] Pisarev R V, Shermatov B N and Nasyrov A 1986 *Sov. Phys.–Solid State* **28** 3338
[21] Di Domenico M and Wemple S H 1969 *J. Appl. Phys.* **40** 720
[22] Burns G and Dacol F H 1981 *Ferroelectrics* **37** 661; 1982 *Solid State Commun.* **42** 9; 1983 *Phys. Rev.* B **28** 2527
[23] Fujii Y and Sakudo T 1970 *J. Appl. Phys.* **41** 4118
[24] Geusic J E, Kurtz S K, Van Uitert L G and Wemple S H 1964 *Appl. Phys. Lett.* **4** 141
[25] Schäfer F J and Kleemann W 1985 *J. Appl. Phys.* **57** 2606
[26] Kleemann W, Schäfer F J, Müller K A and Bednorz J G 1988 *Ferroelectrics* **80** 297
[27] Nye J F 1979 *Physical Properties of Crystals* (Oxford: Clarendon) p 235